OLYMPUS

THIS IS NOT **BEER.**

This is an ethanol dewetting pattern on a glass-air interface captured with a 10X X Line objective.

Image: © Karl Gaff

Breaking barriers in optical performance.

See the truth with Olympus X Line

Scan the code to discover more.

X LINE

Contact your Olympus sales representative or visit **www.olympus-lifescience.com/307-xline** to learn more.

Received: 15 April 2021 | Revised: 19 July 2021 | Accepted: 15 November 2021

DOI: 10.1002/jemt.24009

RESEARCH ARTICLE

MICROSCOPY RESEARCH & TECHNIQUE WILEY

Zona Pellucida sperm-binding protein 3 receptor distribution during *Gopc*$^{-/-}$ globozoospermic spermatogenesis

Maider Bizkarguenaga[1] | **Laura Gomez-Santos**[1] | **Juan Francisco Madrid**[2] | **Francisco José Sáez**[1] | **Edurne Alonso**[3]

[1]Department of Cell Biology and Histology, School of Medicine and Nursing, University of the Basque Country (UPV/EHU), Leioa, Spain

[2]Department of Cell Biology and Histology, School of Medicine, University of Murcia, Murcia, Spain

[3]Department of Cell Biology and Histology, Faculty of Pharmacy University of the Basque Country (UPV/EHU), Vitoria-Gasteiz, Spain

Correspondence
Edurne Alonso, Department of Cell Biology and Histology, Faculty of Pharmacy University of the Basque Country (UPV/EHU) Vitoria-Gasteiz, Spain.
Email: edurne.alonso@ehu.eus

Funding information
UPV/EHU, Grant/Award Numbers: UFI 11/44, EHUA13/15

Review Editor: Paolo Bianchini

Abstract

Globozoospermia is a type of teratozoospermia characterized by round morphology of the sperm head. *Gopc*$^{-/-}$ infertile globozoospermic murine model has failures during spermiogenesis, such as the incorrect biogenesis of the acrosome, disorganized acroplaxome and manchette, round nuclei and spiral flagella. In this study, Western blot, RT-PCR, immunohistochemistry and immunogold were done for the localization of the acrosome protein Zona Pellucida sperm-binding protein 3 receptor (ZP3R), also called sp56, in wild type and *Gopc*$^{-/-}$ mice testis. The ZP3R protein was located in the acrosome and pseudo-acrosome vesicles of wild type and *Gopc*$^{-/-}$ mice, respectively. Also, it is distributed through the cytoplasm of the haploid spermatids only. The incorrect spermiogenesis of *Gopc*$^{-/-}$ mice causes a deregulation in the expression of ZP3R in the globozoospermic spermatids. Our results suggest that although the lack of GOPC causes a failure during the transport of the pre-acrosomal vesicles, the acrosome protein ZP3R is localized in the acrosome and is distributed through the cytoplasm only during spermiogenesis. Furthermore, the failure in spermiogenesis does not impair the synthesis of ZP3R and its localization in the pre-acrosomal vesicles.

KEYWORDS
acrosome, globozoospermia, GOPC, pseudoacrosome, Sp56, spermiogenesis, ZP3R

1 | INTRODUCTION

The acrosome develops during spermiogenesis, the process in which the round spermatids differentiate into sperm-shape cells. In the Golgi phase, the Golgi apparatus forms the pre-acrosomal vesicles which are transported to the anterior part of the nucleus, where they fuse with each other and attach to the nuclear envelope by means of the acroplaxome, an F-actin containing cytoskeletal plate that develops between the acrosome and the nuclear envelope (Anakwe, Sharma, Hoff, Hardy, & Gerton, 1991; Kierszenbaum, Rivkin, & Tres, 2003; Ramalho-Santos, Moreno, Wessel, Chan, & Schatten, 2001). In the cap phase, the pre-acrosomal vesicles form a single round acrosomal vesicle and this vesicle spreads over the anterior half of the nucleus at the time that new pre-acrosomal vesicles fuse. In the elongation phase, both the acrosomal sac and the nucleus elongate by the action of the acrosome–acroplaxome–manchette complex, a transient microtubule and F-actin-containing cytoskeletal dynamic complex, formed by these structures that work together (Kierszenbaum et al., 2003). In the maturation phase, the acrosomal granule, formed by soluble proteins spreads over the entire acrosome (reviewed in Ito &

Toshimori, 2016). The transport of pre-acrosomal vesicles from the Golgi apparatus to the anterior part of the nucleus is produced by motor proteins, such as kinesin and dynein, associated with microtubules, and myosin-Va protein, coupled with actin filaments (Kierszenbaum & Tres, 2004). The Kinesin-like protein (KIFC1) motor protein has been described during the microtubule transport of the pre-acrosomal vesicles from the Golgi apparatus to the acrosome (Yang & Sperry, 2003). A key role for myosin-Va protein has also been suggested. This protein is located in the pre-acrosomal vesicles by interaction with its receptor Rab27a/b and participates, first, in the transport from Golgi to acrosome by actin filaments, and later, in the anchoring of the acrosomal sac to the acroplaxome (Hayasaka et al., 2008).

These studies suggest two routes of transport of the pre-acrosomal vesicles to the acroplaxome, but a third route has also been proposed, which involves the delivery of vesicles from the lysosomal pathway to the acrosome (revision in Berruti & Paiardi, 2011). This third route is supported by the location of the non-proteolytic Ubiquitin carboxyl-terminal hydrolase 8 (mUBPy) ubiquitinating protein, together with its receptor Tyrosine-protein kinase Met (MET), in the membrane of some pre-acrosomal vesicles and in the acrosome during all the formation phases (Berruti & Paiardi, 2015). The mUBPy protein regulates the formation of endosomes in the lysosomal pathway, as well as its microtubule-mediated transport (Bose, Manku, Culty, & Wing, 2014; Nakamura, 2013). Interestingly, it has been reported that the KIFC1 and Rab27a proteins are also associated with the lysosomal pathway (Mukhopadhyay et al., 2011; Raposo, Marks, & Cutler, 2007).

Sometimes sperm biogenesis does not occur properly, and this is one of the main causes of male infertility. One of these disorders is globozoospermia, characterized by round-headed spermatozoa with an absent or disrupted acrosome, an aberrant nuclear envelope, midpiece defects and spiral morphology of flagella (Dam et al., 2007; Ito et al., 2004; Yao et al., 2002). Some infertile knockout animal models have been used to understand the spermiogenesis process and to identify the molecular machinery involved in sperm head formation, like *Csnk2a2* (Escalier, Silvius, & Xu, 2003; Xu, Toselli, Russell, & Seldin, 1999), *Gopc* (Yao et al., 2002), *Pafah1b1* (formerly *Lis1*) (Nayernia et al., 2003), *Spata1* (Dam et al., 2007), *Pick* (Xiao et al., 2009), *DPY19L2* (Harbuz et al., 2011), *Atg* (Wang et al., 2014), *Hrb* (Kang-Decker, Mantchev, Juneja, McNiven, & van Deursen, 2001) or *GM13* (Han et al., 2017).

In this study we have analyzed a murine knockout model for *Gopc*. During spermatogenesis Golgi-associated PDZ and coiled-coil motif-containing protein or GOPC is initially located in the trans-Golgi network of the spermatocytes, then in round spermatids, and finally in elongated spermatids, in which it is less abundant in the trans-Golgi region than in the rest of the cytoplasm (Yao et al., 2002). Moreover, GOPC is also located in others cell types, that is, pancreatic β-cells, with an important role in the pathway required for insulin secretion at the level of trans-Golgi sorting (Wilhelmi et al., 2021). In the male germ line, GOPC is involved in the biogenesis of the acrosome during the transport of pre-acrosomal vesicles from the Golgi apparatus to the perinuclear region and its fusion with the acrosome vesicle.

Gopc$^{-/-}$ spermatids develop a pseudoacrosome formed by several independent small vesicles that do not attach to the acroplaxome (Kierszenbaum, Tres, Rivkin, Kang-Decker, & van Deursen, 2004; Yao et al., 2002). The manchette cytoskeleton is not properly formed either (Lehti & Sironen, 2016).

The mature acrosome contains hydrolytic enzymes and zona pellucida (ZP) recognizing-proteins (Toshimori & Eddy, 2014). One of these recognition proteins is Zona Pellucida sperm-binding protein 3 receptor (ZP3R or Sp56), which binds to the Zona Pellucida sperm-binding protein 3 (ZP3) during fertilization (Bleil & Wassarman, 1990; Cheng et al., 1994) which is initially expressed in the pachytene spermatocytes and continues throughout spermiogenesis. This protein undergoes post-translational modifications during its Golgi apparatus maturation (Kim, Cha, & Gerton, 2001).

Our aim was the ultrastructural localization for the first time of the sperm protein ZP3R during the spermiogenesis of *Gopc*$^{-/-}$ globozoospermic mice; also in wild type mice, to obtain more information about its role in acrosome formation.

2 | MATERIALS AND METHODS

2.1 | Ethics

The experimental procedures involving animals were approved by the Regional Government of Bizkaia and the Ethics Committee for Animal Experimentation (CEEA) of the University of the Basque Country (UPV/EHU), with the number M20/2015/114.

2.2 | Animals

Three adult wild type mice (C57BL/6) between 8 and 12 weeks, reared under specific pathogen free conditions, were provided by the Animal Facility Service-SGIker of the University of the Basque Country (Leioa, Spain). These animals were kept under 12-hour conditions of light/dark, as well as water and food ad libitum. Three *Gopc* knockout mice (No. RBRC01253) were provided by the RIKEN BRC, through the National Bio-Resources Project of the MEXT, Japan, with the consent of Professor Tetsuo Noda of the Japanese Foundation for Cancer Research (JFCR), Japan. Testes were dissected immediately after cervical dislocation euthanasia.

2.3 | Immunohistochemistry

Immunohistochemical studies were performed to localize ZP3R protein in testicular sections of wild type and *Gopc*$^{-/-}$ adult mice. Three testes of each were fixed in Bouin's Solution and embedded in paraffin. Tissue sections of 4 μm were made by a Thermo Scientific Sharper Finesse microtome and placed on slides previously treated with poli-L-Lysine

(P8920, Sigma). Antigen retrieval was performed using a Heated Antigen Retrieval 1× (Abcam) in phosphate buffer saline (PBS), at 98°C in a Kendro HERAhibrid 6 oven for 20 min. The endogenous peroxidase was blocked with 3% H_2O_2 in PBS and then the unspecific antibody binding was blocked by incubation with bovine serum albumin (BSA) at 1 mg/ml, and 10% Normal Goat Serum for 1 hr. Then, the immunohistochemical procedure was carried out on three samples of each testis as follows. The samples were incubated with the Mouse Sperm Protein sp56 Monoclonal primary antibody (55101, QED BioScience), at 13.4 μg/ml with the same blocking medium overnight at 4°C. Sections incubated with the blocking medium without the primary antibody were used as a negative control. Then, the samples were incubated with the Goat Anti-mouse-HRP secondary antibody (A0412, Sigma-Aldrich) at 10 μg/ml and the labeling was visualized by 3,3′-diaminobenzidine (DAB) as chromogen. The sections were counterstained with Meyer's hematoxylin, dehydrated and mounted with DPX mounting medium. All images were examined and captured using Olympus BX50 optical microscopy (Olympus Optical Co., Tokyo, Japan), with the Cell^A Software (Olympus Soft Imaging Solutions).

2.4 | RNA extraction and real-time quantitative PCR analysis

Total RNA was extracted from the Bouin fixed and paraffin-embedded samples of C57BL/6 and *Gopc*$^{-/-}$ mice using the FFPE RNA Purification Kit (NorgenBiotek Corp.) following the manufacturer's instructions. cDNA was obtained by reverse transcription of extracted RNA using the iScript cDNA Kit (BIO-RAD), following the manufacturer's guide. The quality of the extracted RNA was assessed around two with a Synergy HT. For retrotranscription, 0.037 μg/μl of RNA was used for each sample. All the primers used were designed with the Primer Designing Tool from public databases (NCBI) under our qPCR experimental conditions. The primers used for *Zp3r* were: forward, 5′-GAATAGTGAGCAGAGGCGCA-3′, and reverse 5′-AGCTTGTACACC TTCAGGGC-3′. 40S Ribosomal Protein S15 (*Rps15*) was used as positive internal control, forward 5′-CCGAGTAACCGCCAAGATGG-3′, and reverse 5′-TTGCTCATAGGACATGTCGA-3′.

Platinum®Multiplex PCR Master Mix 2× Kit (Applied Biosystems) was carried out with the following reagents: cDNA (0.2 μg), Platinum® Multiplex PCR Master Mix (1×), primers (50 nM) and Nuclease Free Water for a total reaction volume of 50 μl. It was used because the cDNA obtained from the paraffin-embedded testis came from fragmented RNA. Quantitative polymerase chain reaction (PCR) was performed with the obtained DNA (diluted 10 times from Multiplex amplification) mixed with 5 μl of Power SYBR® Green PCR Master Mix (Applied Biosystems), 1 μl of primers (0.5 μM) and Nuclease Free water for a total reaction volume of 10 μl. The samples were amplified in an CFX96™ (BIO-RAD) as follows: an initial step at 95°C for 10 min, followed by 40 cycles of 95°C for 15 s and 60°C for 60 s. Quantitative PCR data were processed by CFX Manager™ software (BIO-RAD). The relative expression of each gene was calculated using the standard $2^{-\Delta Ct}$ method (Schmittgen & Livak, 2008), normalized to the internal control gene *Rps15*.

2.5 | Western blot

Wild type and *Gopc*$^{-/-}$ mice testes were homogenized in 300 μl/sample RIPA Lysis Buffer (Sigma-Aldrich) with a cocktail of Proteinases Inhibitors (Sigma-Aldrich) for 20 min. Then, samples (300 μl) were sonicated with a Sonoplus Ultrasonic Homogenizer (Bandelin) as follows: sonication with 100% amplitude for 10 s, a break of 10 s in ice, and another sonication with 100% amplitude for 10 s. Protein quantification was done with the Bicinconinic acid method (BCA method). Prior to the application to the samples in the gels, they were suspended in Morris Buffer 1× (625 μl Tris–HCl 1 M, 0.25 g SDS, 0.2 ml of 0.1% bromophenol blue, 1 ml glycerine, 0.5 ml β-mercaptoethanol). Testis samples were separated by electrophoresis in a 10% SDS-PAGE gel, under non-denaturing and reducing conditions, and then electrotransferred to nitrocellulose membranes using a transfer buffer (3 g Tris, 14.2 g glycine, 1 g SDS, 200 ml methanol, 700 ml ultrapure water) and 0.6A constant amperage for 3 hr at 4°C. The membranes were then incubated in 5% (wt/vol) bovine serum albumina (BSA) and incubated with Mouse Sperm Protein sp56 Monoclonal primary antibody (5510, QED Bioscience) at 4 μg/ml, overnight at 4°C. The secondary anti-mouse-HRP antibody (S2004, Santa Cruz) was used at 0.2 μg/ml. The blotting membranes were developed with Luminata™ Crescendo Western HRP Substrate in a G:BOX (Syngene) according to the manufacturer's instructions and the images were obtained with the GeneSnap Software. The internal control used was anti-α-tubulin primary antibody (T5168, Sigma-Aldrich) at 1.5 μg/ml, in the same conditions as previously described. The same exposure times were used on all samples when comparing different membranes.

2.6 | Immunogold

Testis samples were cut into small pieces of average 1 mm^3 and fixed with 2% glutaraldehyde in PBS (Varndell & Polak, 1987). After that, samples were incubated with 0.5 M NH_4Cl for 1 hr to block aldehyde groups. Then, they were embedded in Lowicryl® K4M (Sigma-Aldrich) following Altman, Schneider, & Papermaster, 1984, protocol. The samples were sectioned at 70 nm using a Leica Ultracut UCT (Leica) ultramicrotome. Two hundred Mesh grids were coated with a 0.25% Formvar Solution (Electron Microscopy Sciences), and then ultrathin sections were mounted on them. The sections were blocked with BSA at 1 mg/ml and 10% Normal Goat Serum for 1 hr and incubated with the Mouse Sperm Protein sp56 Monoclonal primary antibody at 0.6 mg/ml, overnight at 4°C and goat anti-mouse 15 nm gold (ab202673, abcam) at 0.34 μg/ml as secondary antibody. The sections were contrasted with Uranil Acetate and Lead Citrate and examined with a Philips EM208S electron microscope in the *Analytical and High-Resolution Microscopy Service* (SGIker) at the University of The Basque

Country (UPV/EHU). All the images were obtained with the Cell^A Software.

2.7 | Statistical analysis

The statistical analysis was performed with the program GraphPad Prism5 (San Diego, CA, USA). Mann–Whitney *U* test was performed to analyze *Zp3r* mRNA relative expression and the relative expression was transformed to relative fold changes of gene expression using the Mean ± SEM. Immunocytochemical expression of ZP3R was analyzed along the spermiogenic cells found in stages I, V, and X of the cycle of the seminiferous epithelium of the wild type and *Gopc*$^{-/-}$ mice. The gold particles were identified by their rounded and fully electrodense appearance of 15 nm diameter. The quantitative analysis of the immunogold labeling was done using the software FIJI (ImageJ) in a total of seven cells for each type of cell. The measurements were done by counting the gold particles in the whole cytoplasm and acrosomes, and measuring the total areas of all of them. These results were given as gold particles/μm^2. The statistical differences of the numerical density of gold particles in cytoplasm and acrosome between each cell type was calculated and analyzed by 2-way ANOVA with Bonferroni's *post hoc* test, using the Mean ± SEM. Statistically significant differences were considered at $p < .05$, $p < .01$, and $p < .001$.

3 | RESULTS

We report here the presence of ZP3R in the acrosome and cytoplasm of the haploid cells of the seminiferous tubules in wild type and in *Gopc* knockout mice.

3.1 | Immunohistochemical localization of ZP3R in *Gopc*$^{-/-}$ and wild type testis

For the description and classification of the different stages and steps of the murine spermatogenesis we followed Russell, Ettlin, Sinha Hikim, and Clegg (1990) protocol of Oakberg's 12-stage scheme.

The distribution pattern analyzed by immunohistochemistry in the wild type and *Gopc*$^{-/-}$spermatogenesis showed that ZP3R was localized exclusively in the cytoplasm and acrosome region of the round and elongated spermatids. Neither spermatogonia nor spermatocytes were stained (Figure 1).

The cytoplasm of spermatids of both wild-type and *Gopc*$^{-/-}$ individuals was ZP3R immunoreactive from step 2 to step 10 (Figure 1a–h). No labeling was observed from step 14 spermatids (Figure 1a–f). Nevertheless, wild type immunostaining of cytoplasm was stronger than in *Gopc*$^{-/-}$ spermatids.

The acrosome region of the samples of both specimens (wild type and *Gopc*$^{-/-}$) showed the same immunoreactivity to ZP3R from step 2 to step 10 spermatids (Figure 1). Nonetheless, spermatids in steps 14 and 15 of the *Gopc*$^{-/-}$ mice showed stronger labeling pattern than the wild type individuals (Figure 1a–d).

3.2 | RT-qPCR

The analysis of the relative gene expression of ZP3R mRNA (Figure 2a) showed significantly higher levels ($p < .001$) in *Gopc*$^{-/-}$ mice than in the wild type. The relative fold changes of gene expression in *Gopc*$^{-/-}$ was increased 12-fold (12.67 ± 0.8609).

3.3 | Western blot analysis

Western blot analysis of total protein extracts from wild-type and *Gopc*$^{-/-}$ mice showed a strong band of about 65 KDa (Figure 2b).

3.4 | Ultrastructural analysis of ZP3R distribution by immunogold

Immunogold was performed in order to analyze the intracellular localization of ZP3R in round and elongated spermatids.

All the spermatids of both wild type (Figure 3) and *Gopc*$^{-/-}$ mice (Figure 4) were immunoreactive to ZP3R in the region of the Golgi apparatus as well as distributed throughout the rest of the cytoplasm. Whereas in wild type ZP3R immunolabeling was higher in the cytoplasm of round spermatids (Figure 3a,b) than the elongated spermatids (Figure 3d,e), in *Gopc*$^{-/-}$ spermatids ZP3R staining seemed to be similar throughout all the spermiogenesis (Figure 4).

In the acrosome of round spermatids the immunoreactivity was similar in both types of mice, but from step 13 spermatid immunolabeling was higher in *Gopc*$^{-/-}$ (Figures 4d,e and 3d,e). These results confirm those obtained with light microscopy immunohistochemistry (Figure 1a–d). Also, the matrix of the acrosomal vesicle and the inner acrosomal membrane were immunoreactive (Figures 3c,d and 4c,d), but never the outer acrosomal membrane.

3.5 | Relative expression of ZP3R in wild type and *Gopc*$^{-/-}$ spermatids

The numerical density of immunogold labeling was analyzed in the whole cytoplasm and in the specific perinuclear region of the acrosome of both wild type and *Gopc*$^{-/-}$ spermatids.

The cytoplasmic labeling density of ZP3R showed no significant difference in C57Bl/6 wild type sample, except in step 9 where it was significantly lower ($p < .05$) (Figure 5a). However, the *Gopc*$^{-/-}$ mice showed a notable and significant increase of expression of ZP3R ($p < .01$) between steps 5 and 13 and onwards (Figure 5b). Comparing the expression of ZP3R in the cytoplasm between the spermatids of wild type and knockout mice, a significant decrease of immunolabeling ($p < .05$) in step 5 spermatids of *Gopc*$^{-/-}$ and a significant labeling

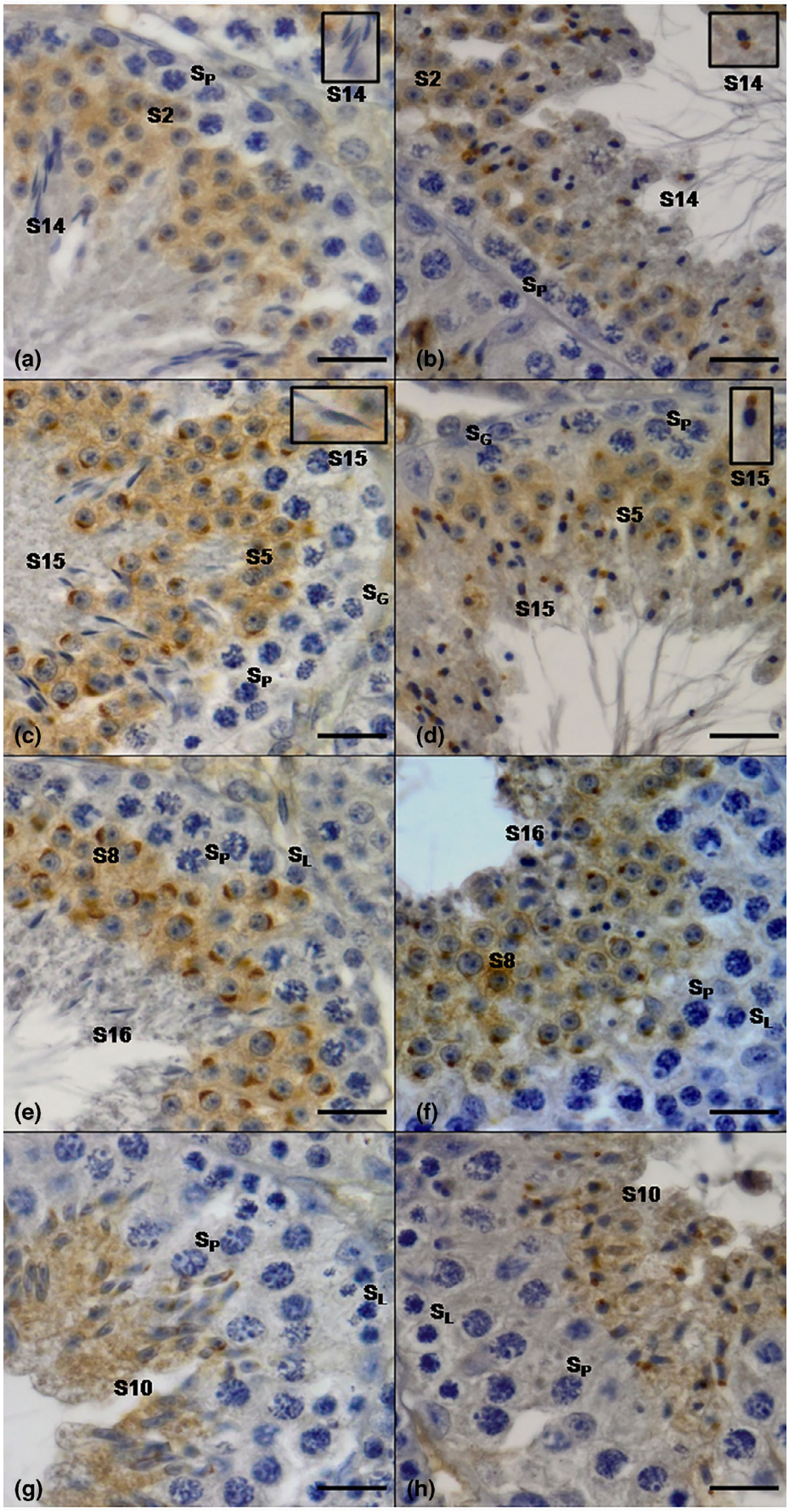

FIGURE 1 Immunohistochemistry of ZP3R protein in mouse testis. Expression of ZP3R in several stages of the cycle of the mouse seminiferous tubules of C57Bl/6 wild type mice: (a) stage II, (b) stage V, (c) stage VIII, and (d) stage X; and *Gopc*$^{-/-}$ mice: (e) stage II, (f) stage V, (g) stage VIII, and (h) stage X. The ZP3R protein was located as brown staining in the acrosome and cytoplasm of the round and elongated spermatids. S_G, spermatogonia; S_L, leptotene spermatocyte; S_P, pachytene spermatocyte; S_2, S_5, S_8, S_{10}, S_{14}, S_{15}, S_{16}: steps of round and elongated spermatids. Scale bar: 20 μm. Detail of the elongated spermatids (steps 14 and 15) in the box on the top right

(a)

CT Zp3r		2^-ΔCT Zp3r (relative expression)		Fold change (KO/WT)
C57BL/6	*Gopc*$^{-/-}$	*C57BL/6*	*Gopc*$^{-/-}$	12,667437
24,45	20,21	0,009486	0,11657	

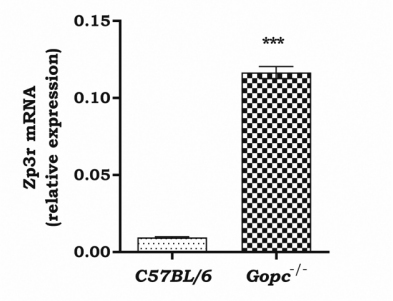

(b)

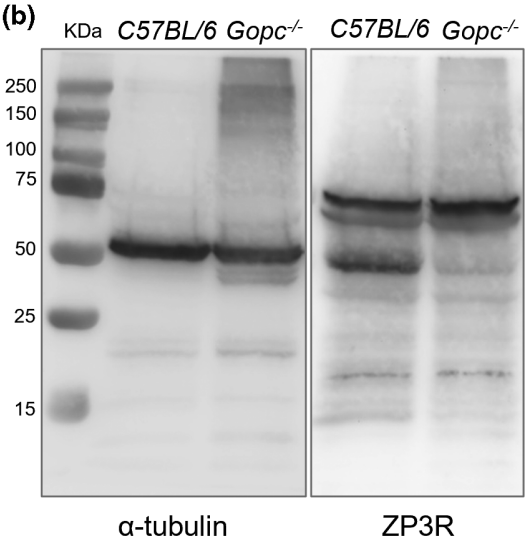

FIGURE 2 Quantitative RT-PCR analysis of *Zp3r* transcript and Western blot of ZP3R expression in C57Bl/6 wild type and *Gopc*$^{-/-}$ mice testis. a) There is an increase in *Zp3r* transcript in the *Gopc*$^{-/-}$ mouse testis. Relative expression of *Zp3r* is represented as the mean ± SEM. Statistical differences were considered at $p < .001$(***), Mann–Whitney *U* test. CT, cycle threshold. (b) Anti-ZP3R recognized by Western blot the 65 KDa in C57Bl/6 wild type and *Gopc*$^{-/-}$ testis. KDa, molecular mass markers. Alpha tubulin was used as the internal control

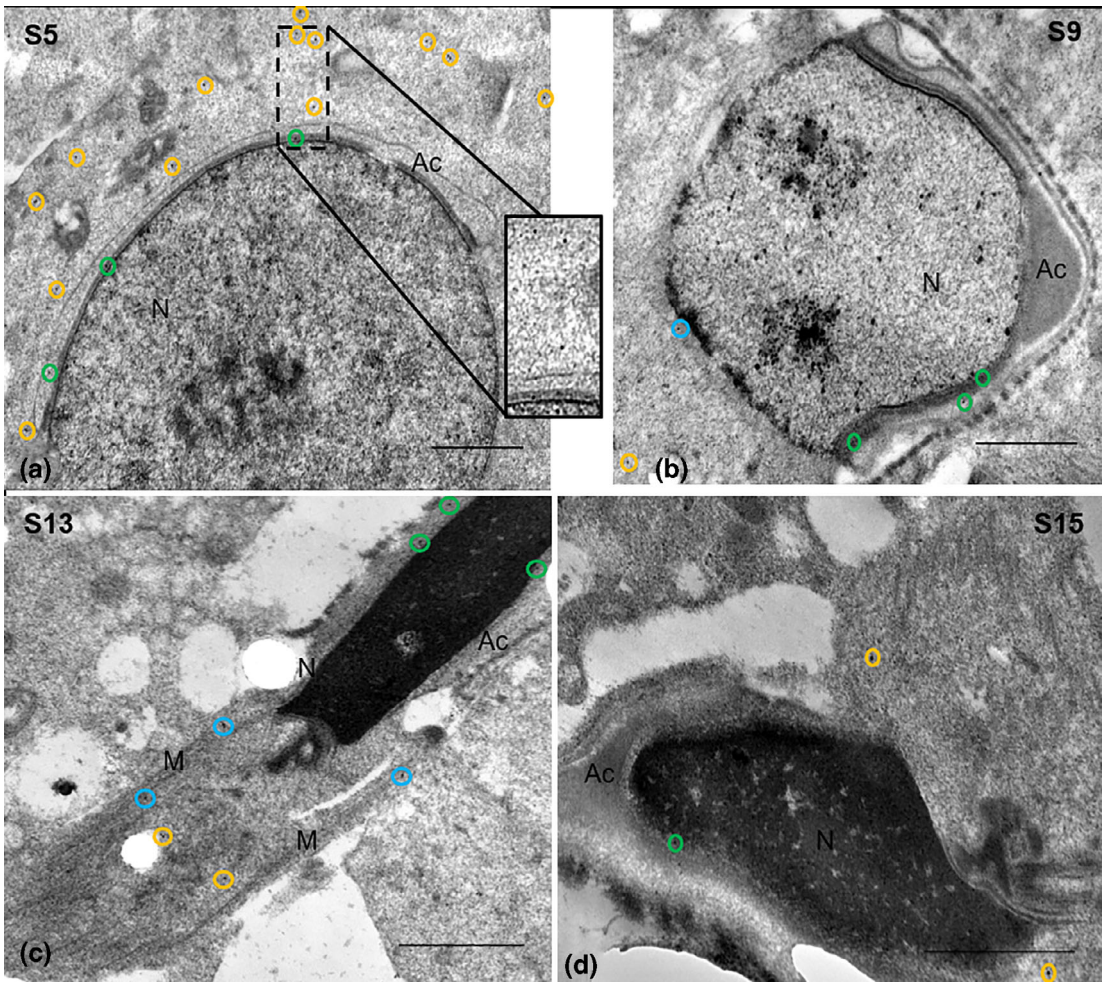

FIGURE 3 Immunogold localization of ZP3R by electron microscopy in C57Bl/6 wild type mouse spermiogenesis. ZP3R were localized in the acrosome region (green circles), manchette (blue circles) and cytoplasm (yellow circles). (a) Round spermatid step 5, (b) elongating spermatid step 9, (c) early elongated spermatid step 13, and (d) elongated spermatid step 15. Ac, acrosome; M, manchette; N, nucleus. Scale bar: 1 μm

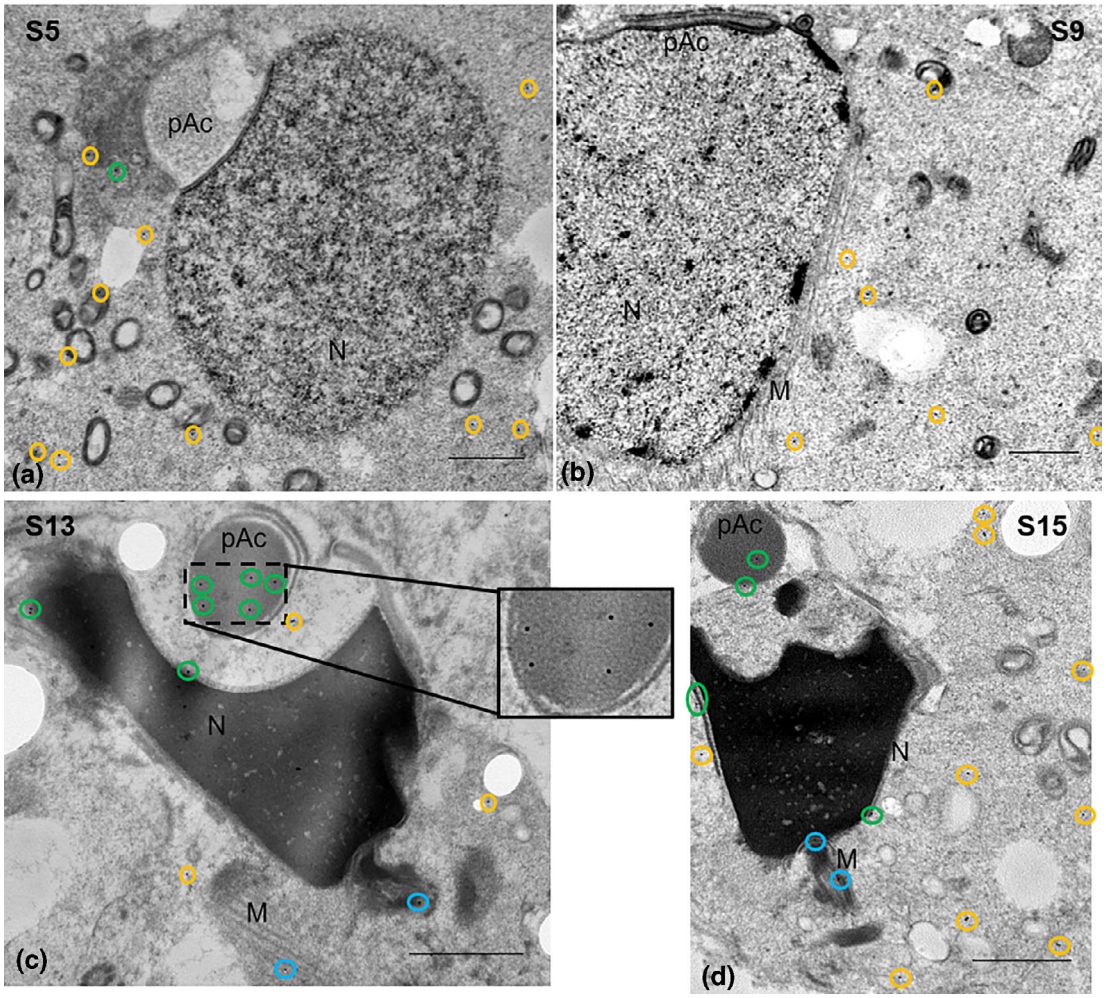

FIGURE 4 Immunogold localization of ZP3R by electron microscopy in *Gopc*$^{-/-}$ mouse spermiogenesis. Labeling was observed in the pseudoacrosome (green circles), cytoplasm (yellow circles) and manchette region (blue circles). (a) Round spermatid step 5, (b) elongating spermatid step 9, (c) early elongated spermatid step 13, and (d) elongated spermatid step 15. pAc, pseudoacrosome; M, manchette; N, nucleus. Scale bar: 1 μm

increase ($p < .05$) in step 15 spermatids of the knockout mice were observed ($p < .05$) (Figure 5c).

The distribution of ZP3R in both the acrosome of the wild type and the pseudoacrosome of *Gopc*−/− mice did not show significant differences; it was almost the same. A significant difference was only observed in step 15 spermatids, where acrosome ZP3R expression was notably higher in the *Gopc*$^{-/-}$ mice (Figure 5d).

4 | DISCUSSION

Spermiogenesis is the last phase of t sperm formation, in which round spermatids develop into elongated sperm through several structural modifications: acrosome biogenesis, nuclear compaction, flagella formation, mitochondrial reorganization and the removal of almost all the cytoplasm. In globozoospermic spermiogenesis these structural modifications are impaired, resulting in the incorrect biogenesis of the acrosome, slow compaction of the chromatin, round nuclei, disorganization of the acroplaxome and manchette and spiral flagella.

For the first time, we have carried out an ultrastructural study to analyze the location of the ZP3R protein, also called sp56, during the spermatogenesis in wild type and *Gopc*$^{-/-}$ globozoospermic mice.

4.1 | ZP3R protein cellular distribution in the seminiferous epithelia in wild type and *Gopc*$^{-/-}$ mice

ZP3R is a protein that labels to ZP3 and is involved in the recognition of the zona pellucida (ZP) during fertilization, the first step before the sperm can penetrate the ZP of the oocyte (Bleil & Wassarman, 1990).

We have localized ZP3R protein by immunohistochemistry distributed in the cytoplasm and in the acrosome of the spermatids of wild type mice. Immunogold results reveal the presence of the protein in the acrosomal sac and the cytoplasm of the spermatids of stages I, V, and X of the seminiferous epithelium. ZP3R was absent in the

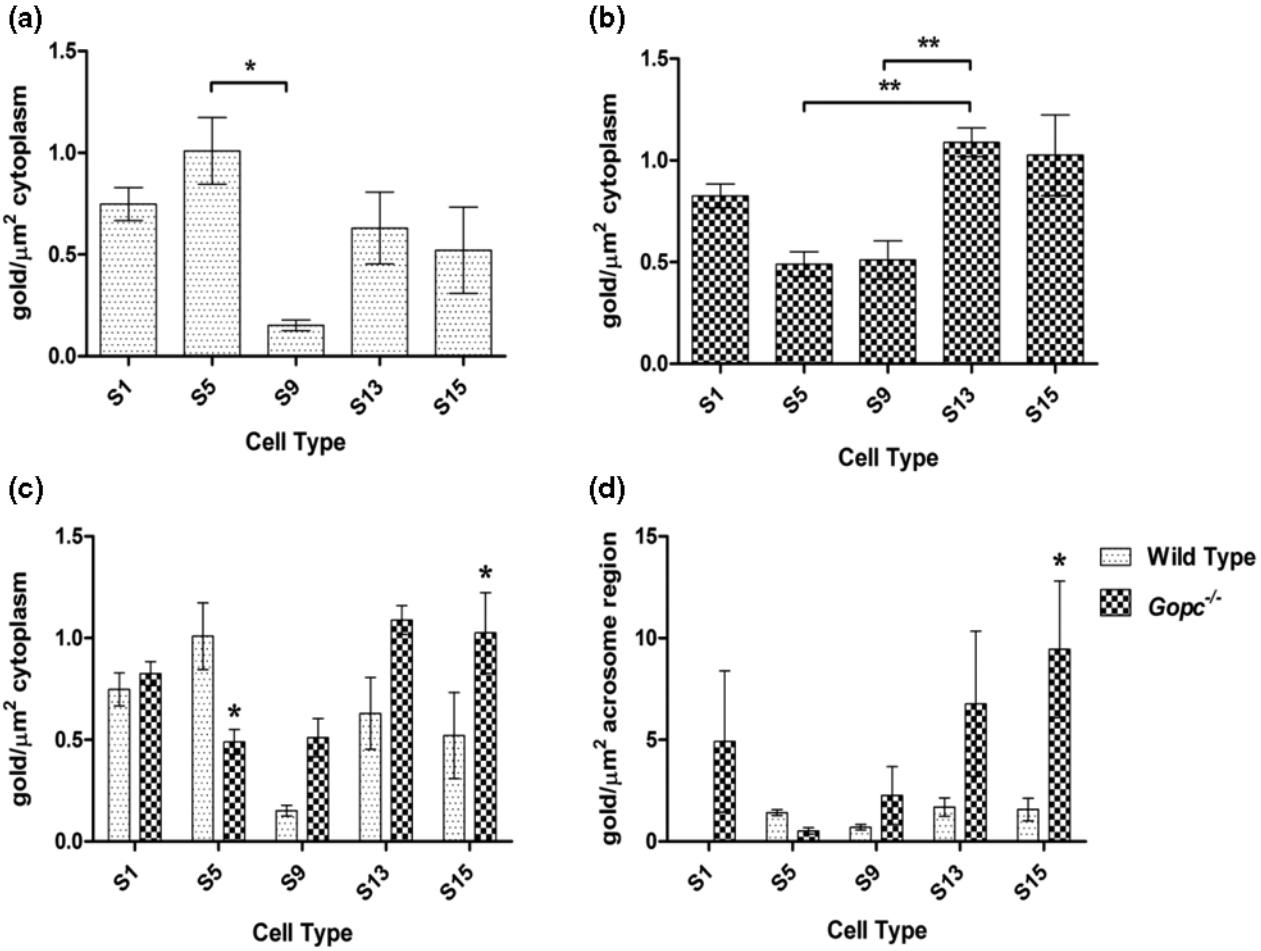

FIGURE 5 Quantitative analysis of the immunogold labeling of ZP3R in the cytoplasm of spermatids. The numerical density of colloidal gold particles was estimated as mean ± SEM of the number of gold particles/μm^2 for the cytoplasm in C57Bl/6 wild type spermatids (a), *Gopc*$^{-/-}$ spermatids (b), and both compared (c) and for the acrosomal region of both mice compared (d). Statistical differences were considered at $p < .05$ (*), $p < .01$(**), two-way ANOVA with Bonferroni's *post hoc* test

spermatogonia and in the spermatocytes, similarly to Bookbinder, Cheng, and Bleil (1995). The synthesis of ZP3R begins at the pachytene phase, as has been described by Western blot (Kim et al., 2001). Nevertheless, according to our results, the localization of ZP3R is exclusive to haploid cells.

The use of a knockout model with a wrong acrosome formation allows us to understand the acrosome biogenesis. Globozoospermic phenotype can be obtained with a single gene mutation of *Gopc* (Yao et al., 2002). GOPC protein has an important role in acrosome biogenesis and its absence results in a multivesicular structure or pseudoacrosome and a defective acroplaxome–manchette complex (Bizkarguenaga, Gomez-Santos, Madrid, Sáez, & Alonso, 2019; Lehti & Sironen, 2016). Our immunogold results revealed the presence of ZP3R protein in the cytoplasm and the pseudoacrosome of all the spermatids of *Gopc*$^{-/-}$ mice.

When we analyzed the localization and expression of ZP3R in the cytoplasm of the spermatids of wild type mice we have seen this protein both in the Golgi apparatus and distributed throughout the cytoplasm. We have also observed that its levels decreased in step 9 spermatids. This could be due to the maturation, segregation, and package of the protein, which would be transported in vesicles to the acrosome. However, this ZP3R-transport pathway from trans-Golgi to acrosome does not explain the wide distribution throughout the cytoplasm. It could be that ZP3R-containing vesicles are stored in the cytoplasm until they are required to form the acrosome, a hypothesis that has been postulated by Berruti & Paiardi, 2011, who indicated that the acrosome is a lysosome related organelle (LRO) formed from a main vesicle, from which the pre-acrosomal vesicles form. This lysosomal pathway for the biogenesis of the acrosome would be combined with the direct pre-acrosome vesicles transport from the Golgi apparatus. There are several data that correlate to this hypothesis. Membrane proteins which belong to the endocytic pathway have also been located in the acrosome, such as the testicular-specific proton pump and the USP/UBPγ protein with its MET membrane receptor (Berruti & Paiardi, 2015; Sun-Wada, Wada, & Futai, 2004). Even the KIFC1 and Rab27a proteins, which are involved in vesicular traffic to the acrosome, have been associated with vesicles related to lysosomes (Mukhopadhyay et al., 2011; Raposo et al., 2007) and with

intracellular vesicular traffic (Harris & Littleton, 2011; Seabra, Mules, & Hume, 2002). Moreno, Ramalho-Santos, Sutovsky, Chan, & Schatten, 2000, have also observed that near the acrosome region there are other vesicles with acid pH, a distinctiveness of lysosomes. Additionally, proteins that are related to this intracellular vesicle transport pathway, such as clathrin, COP (Moreno, Ramalho-Santos, Chan, Wessel, & Schatten, 2000), and SNARE (Ramalho-Santos et al., 2001) have been located in these pre-acrosomal vesicles. These data should be taken into account.

4.2 | ZP3R expression dynamics in the acrosome region

The Western blot analysis of total testicular extract of wild type and knockout mice showed a strong band at 65 KDa, as described in the literature (Buffone, Kim, Doak, Rodriguez-Miranda, & Gerton, 2009; Kim et al., 2001), without appreciable differences between wild type and knockout mice. However, it has been previously shown that the concentration of ZP3R increases during spermatogenesis getting a maximum peak of concentration in protein extract from mature sperm (Kim et al., 2001).

Our immunohistochemical and immunogold results showed an exclusive distribution of ZP3R in the cytoplasm and in the acrosome of wild type or pseudoacrosome of *Gopc*$^{-/-}$ mice, which suggests that the synthesis and distribution of ZP3R is not impaired in globozoospermic spermiogenesis. In contrast, our quantitative RT-PCR results show that the expression of ZP3R protein is also unregulated, like other proteins studied during the spermatogenesis, such as the acrosome protein Germ cell nuclear factor (GCNF) in *Gopc*$^{-/-}$ (Bizkarguenaga et al., 2019). Moreover, we observed that the gene expression of this protein was 12-times higher in the *Gopc*$^{-/-}$ seminiferous epithelium. This could be explained because the *Gopc*$^{-/-}$ mice are affected in the elongation of the spermatid head resulting in less chromatin condensation that might facilitate the gene expression of ZP3R in these knockout mice.

The labeling density of ZP3R in the cytoplasm of the wild type and the *Gopc*$^{-/-}$ spermatids differed: there is less expression of ZP3R in the cytoplasm of step 5 and higher in step 15 in knockout spermatids, maybe due to the increased number of pre-acrosome vesicles in the cytoplasm that did not assemble into the final acrosome. We observed that the concentration dynamics of ZP3R in pseudoacrosomes of *Gopc*$^{-/-}$ mice is higher than in the acrosomes of wild type mice, although statistical differences are only observable in step 15 spermatids, in accordance with its concentration peak.

At the end of spermiogenesis, most of the cytoplasm of wild type spermatids is fully removed from the sperm cells. However, in the *Gopc*$^{-/-}$ mice the excess of cytoplasm is not correctly removed, as in the *Zpbp1*$^{-/-}$ mice (Lin, Roy, Yan, Burns, & Matzuk, 2007), probably due to wrongly developed cell junctions with Sertoli cells (Ito et al., 2004; Lu, Stewart, & Wilson, 2015). Then, the accumulation of ZP3R could be due to the fact that the mature globozoospermic spermatids have as much cytoplasm as the spermatids of previous stages, so the cellular signals they receive are similar to previous cell types, which causes the translation of this protein while it is still active (Greenbaum, Colangelo, Williams, & Gerstein, 2003).

In conclusion, our data indicate that the acrosome protein ZP3R is only expressed in the haploid cells of the seminiferous epithelium cycle, not only localized specifically in the acrosome, but also distributed through the cytoplasm. In addition, the lack of GOPC, which causes a globozoospermic spermiogenesis, does not impair the synthesis of ZP3R.

ACKNOWLEDGEMENTS

Mrs. C. Tobillas and Mrs. M.J. Fernández contributed to sample preparation. We thank Mrs. M.J. Aldasoro for her support in the office work. This work was supported by grants from the UPV/EHU (EHUA13/15 and UFI 11/44).

DATA AVAILABILITY STATEMENT

The data that support the findings of this study are available from the corresponding author upon reasonable request.

REFERENCES

Altman, L. G., Schneider, B. G., & Papermaster, D. S. (1984). Rapid embedding of tissues in Lowicryl K4M for immunoelectron microscopy. *The Journal of Histochemistry and Cytochemistry*, *32*, 1217–1223. https://doi.org/10.1177/32.11.6436366

Anakwe, O. O., Sharma, S., Hoff, H. B., Hardy, D. M., & Gerton, G. L. (1991). Maturation of Guinea pig sperm in the epididymis involves the modification of proacrosin oligosaccharide side chains. *Molecular Reproduction and Development*, *29*, 294–301. https://doi.org/10.1002/mrd.1080290313

Berruti, G., & Paiardi, C. (2011). Acrosome biogenesis. Revisiting old questions to yield new insights. *Spermatogenesis*, *1*, 95–98. https://doi.org/10.4161/spmg.1.2.16820

Berruti, G., & Paiardi, C. (2015). USP8/UBPγ-regulated sorting and the development of sperm acrosome: The recruitment of MET. *Reproduction*, *149*, 633–644. https://doi.org/10.1530/REP-14-0671

Bizkarguenaga, M., Gomez-Santos, L., Madrid, J. F., Sáez, F. J., & Alonso, E. (2019). Increase of germ cell nuclear factor expression in globozoospermic *Gopc*$^{-/-}$ knockout mice. *Andrology*, *7*, 319–328. https://doi.org/10.1111/andr.12594

Bleil, J. D., & Wassarman, P. M. (1990). Identification of a ZP3-binding protein on acrosome-intact mouse sperm by photoaffinity crosslinking. *Proc Natl Acad Sci USA*, *87*, 5563–5567. https://doi.org/10.1073/pnas.87.14.5563

Bookbinder, L. H., Cheng, A., & Bleil, J. D. (1995). Tissue- and species-specific expression of sp56, a mouse sperm fertilization protein. *Science*, *269*, 86–89. https://doi.org/10.1126/science.7604284

Bose, R., Manku, G., Culty, M., & Wing, S. S. (2014). Ubiquitin–proteasome system in spermatogenesis. *Advances in Experimental Medicine and Biology*, *759*, 181–213. https://doi.org/10.1007/978-1-4939-0817-2_9

Buffone, M. G., Kim, K.-S., Doak, B. J., Rodriguez-Miranda, E., & Gerton, G. L. (2009). Functional consequences of cleavage, dissociation and exocytotic release of ZP3R, a C4BP-related protein, from the mouse sperm acrosomal matrix. *Journal of Cell Science*, *122*, 3153–3160. https://doi.org/10.1242/jcs.052977

Cheng, A., Le, T., Palacios, M., Bookbinder, L. H., Wassarman, P. M., Suzuki, F., & Bleil, J. D. (1994). Sperm-egg recognition in the mouse: Characterization of sp56, a sperm protein having specific affinity for

ZP3. *The Journal of Cell Biology*, *125*, 867–878. https://doi.org/10.1083/jcb.125.4.867

Dam, A. H., Koscinski, I., Kremer, J. A., Moutou, C., Jaeger, A.-S., Oudakker, A. R., … Viville, S. (2007). Homozygous mutation in SPATA16 is associated with male infertility in human globozoospermia. *American Journal of Human Genetics*, *81*, 813–820. https://doi.org/10.1086/521314

Escalier, D., Silvius, D., & Xu, X. (2003). Spermatogenesis of mice lacking CK2alpha': Failure of germ cell survival and characteristic modifications of the spermatid nucleus. *Molecular Reproduction and Development*, *66*, 190–201. https://doi.org/10.1002/mrd.10346

Greenbaum, D., Colangelo, C., Williams, K., & Gerstein, M. (2003). Comparing protein abundance and mRNA expression levels on a genomic scale. *Genome Biology*, *4*, 117. https://doi.org/10.1186/gb-2003-4-9-117

Han, F., Liu, C., Zhang, L., Chen, M., Zhou, Y., Qin, Y., … Gao, F. (2017). Globozoospermia and lack of acrosome formation in GM130-deficient mice. *Cell Death & Disease*, *8*, e2532. https://doi.org/10.1038/cddis.2016.414

Harbuz, R., Zouari, R., Pierre, V., Ben Khelifa, M., Kharouf, M., Coutton, C., … Ray, P. F. (2011). A recurrent deletion of DPY19L2 causes infertility in man by blocking sperm head elongation and acrosome formation. *American Journal of Human Genetics*, *88*, 351–361. https://doi.org/10.1016/j.ajhg.2011.02.007

Harris, K. P., & Littleton, J. T. (2011). Vesicle trafficking: A Rab family profile. *Current Biology*, *21*, R841–R843. https://doi.org/10.1016/j.cub.2011.08.061

Hayasaka, S., Terada, Y., Suzuki, K., Murakawa, H., Tachibana, I., Sankai, T., … Okamura, K. (2008). Intramanchette transport during primate spermiogenesis: Expression of dynein, myosin Va, motor recruiter myosin Va, VIIa-Rab27a/b interacting protein, and Rab27b in the manchette during human and monkey spermiogenesis. *Asian Journal of Andrology*, *10*, 561–568. https://doi.org/10.1111/j.1745-7262.2008.00392.x

Ito, C., Suzuki-Toyota, F., Maekawa, M., Toyama, Y., Yao, R., Noda, T., & Toshimori, K. (2004). Failure to assemble the peri-nuclear structures in GOPC deficient spermatids as found in round-headed spermatozoa. *Archives of Histology and Cytology*, *67*, 349–360. https://doi.org/10.1679/aohc.67.349

Ito, C., & Toshimori, K. (2016). Acrosome markers of human sperm. *Anatomical Science International*, *91*, 128–142. https://doi.org/10.1007/s12565-015-0323-9

Kang-Decker, N., Mantchev, G. T., Juneja, S. C., McNiven, M. A., & van Deursen, J. M. (2001). Lack of acrosome formation in Hrb-deficient mice. *Science*, *294*, 1531–1533. https://doi.org/10.1126/science.1063665

Kierszenbaum, A. L., Rivkin, E., & Tres, L. L. (2003). Acroplaxome, an F-actin-keratin-containing plate, anchors the acrosome to the nucleus during shaping of the spermatid head. *Molecular Biology of the Cell*, *14*, 4628–4640. https://doi.org/10.1091/mbc.e03-04-0226

Kierszenbaum, A. L., & Tres, L. L. (2004). The acrosome-acroplaxome-manchette complex and the shaping of the spermatid head. *Archives of Histology and Cytology*, *67*, 271–284. https://doi.org/10.1679/aohc.67.271

Kierszenbaum, A. L., Tres, L. L., Rivkin, E., Kang-Decker, N., & van Deursen, J. M. A. (2004). The acroplaxome is the docking site of Golgi-derived myosin Va/Rab27a/b- containing proacrosomal vesicles in wild-type and Hrb mutant mouse spermatids. *Biology of Reproduction*, *70*, 1400–1410. https://doi.org/10.1095/biolreprod.103.025346

Kim, K. S., Cha, M. C., & Gerton, G. L. (2001). Mouse sperm protein sp56 is a component of the acrosomal matrix. *Biology of Reproduction*, *64*, 36–43. https://doi.org/10.1095/biolreprod64.1.36

Lehti, M. S., & Sironen, A. (2016). Formation and function of the manchette and flagellum during spermatogenesis. *Reproduction*, *151*, R43–R54. https://doi.org/10.1530/REP-15-0310

Lin, Y.-N., Roy, A., Yan, W., Burns, K. H., & Matzuk, M. M. (2007). Loss of zona pellucida binding proteins in the acrosomal matrix disrupts acrosome biogenesis and sperm morphogenesis. *Molecular and Cellular Biology*, *27*, 6794–6805. https://doi.org/10.1128/MCB.01029-07

Lu, R., Stewart, L., & Wilson, J. M. (2015). Scaffolding protein GOPC regulates tight junction structure. *Cell and Tissue Research*, *360*, 321–332. https://doi.org/10.1007/s00441-014-2088-1

Moreno, R. D., Ramalho-Santos, J., Chan, E. K., Wessel, G. M., & Schatten, G. (2000). The Golgi apparatus segregates from the lisosomal/acrosomal vesicle during rhesus spermiogenesis: Structural alterations. *Developmental Biology*, *219*, 334–349. https://doi.org/10.1006/dbio.2000.9606

Moreno, R. D., Ramalho-Santos, J., Sutovsky, P., Chan, E. K., & Schatten, G. (2000). Vesicular traffic and Golgi apparatus dynamics during mammalian spermatogenesis: Implications for acrosome architecture. *Biology of Reproduction*, *63*, 89–98. https://doi.org/10.1095/biolreprod63.1.89

Mukhopadhyay, A., Nieves, E., Che, F. Y., Wang, J., Jin, L., Murray, J. W., … Wolkoff, A. W. (2011). Proteomic analysis of endocytic vesicles: Rab1a regulates motility of early endocytic vesicles. *Journal of Cell Science*, *124*, 765–775. https://doi.org/10.1242/jcs.079020

Nakamura, N. (2013). Ubiquitination regulates the morphogenesis and function of sperm organelles. *Cell*, *2*, 732–750. https://doi.org/10.3390/cells2040732

Nayernia, K., Vauti, F., Meinhardt, A., Cadenas, C., Schweyer, S., Meyer, B. I., … Arnold, H.-H. (2003). Inactivation of a testis-specific Lis1 transcript in mice prevents spermatid differentiation and causes male infertility. *The Journal of Biological Chemistry*, *278*, 48377–48385. https://doi.org/10.1074/jbc.M309583200

Ramalho-Santos, J., Moreno, R. D., Wessel, G. M., Chan, E. K., & Schatten, G. (2001). Membrane trafficking machinery components associated with the mammalian acrosome during spermiogenesis. *Experimental Cell Research*, *267*, 45–60. https://doi.org/10.1006/excr.2000.5119

Raposo, G., Marks, M. S., & Cutler, D. F. (2007). Lysosome-related organelles: Driving post-Golgi compartments into specialization. *Current Opinion in Cell Biology*, *19*, 394–401. https://doi.org/10.1016/j.ceb.2007.05.001

Russell, L. D., Ettlin, R. A., Sinha Hikim, A. P., & Clegg, E. D. (1990). *Histological and histopathological evaluation of the testis* (p. 286). Clearwater: Cache River XIV.

Schmittgen, T. D., & Livak, K. J. (2008). Analyzing real-time PCR data by the comparative C(T) method. *Nature Protocols*, *3*, 1101–1108. https://doi.org/10.1038/nprot.2008.73

Seabra, M. C., Mules, E. H., & Hume, A. N. (2002). Rab GTPases, intracellular traffic and disease. *Trends in Molecular Medicine*, *8*, 23–30. https://doi.org/10.1016/s1471-4914(01)02227-4

Sun-Wada, G.-H., Wada, Y., & Futai, M. (2004). Diverse and essential roles of mammalian vacuolar-type proton pump ATPase: Toward the physiological understanding of inside acidic compartments. *Biochimica et Biophysica Acta*, *1658*, 106–114. https://doi.org/10.1016/j.bbabio.2004.04.013

Toshimori, K., & Eddy, E. M. (2014). The spermatozoon. In T. M. Plant & A. J. Zeleznik (Eds.), *Knobil and Neill's physiology of reproduction* (Vol. 1, 4th ed., pp. 99–148). San Diego: Academic Press.

Varndell, I. M., & Polak, J. M. (1987). EM immunolabeling. In J. Sommerville & U. Scheer (Eds.), *Electron microscopy in molecular biology: A practical approach*. Oxford. United Kingdom: IRL Press.

Wang, H., Wan, H., Li, X., Liu, W., Chen, Q., Wang, Y., … Li, W. (2014). Atg7 is required for acrosome biogenesis during spermatogenesis in mice. *Cell Research*, *24*, 852–869. https://doi.org/10.1038/cr.2014.70

Wilhelmi, I., Grunwald, S., Gimber, N., Popp, O., Dittmar, G., Arumughan, A., … Schürmann, A. (2021). The ARFRP1-dependent Golgi scaffolding protein GOPC is required for insulin secretion from pancreatic β-cells. *Mol Metab*, *45*, 101151. https://doi.org/10.1016/j.molmet.2020.101151

Xiao, N., Kam, C., Shen, C., Jin, W., Wang, J., Lee, K. M., … Xia, J. (2009). PICK1 deficiency causes male infertility in mice by disrupting

acrosome formation. *The Journal of Clinical Investigation*, *119*, 802–812. https://doi.org/10.1172/JCI36230

Xu, X., Toselli, P. A., Russell, L. D., & Seldin, D. C. (1999). Globozoospermia in mice lacking the casein kinase II alpha' catalytic subunit. *Nature Genetics*, *23*, 118–121. https://doi.org/10.1038/12729

Yang, W.-X., & Sperry, A. O. (2003). C-terminal kinesin motor KIFC1 participates in acrosome biogenesis and vesicle transport. *Biology of Reproduction*, *69*, 1719–1729. https://doi.org/10.1095/biolreprod.102.014878

Yao, R., Ito, C., Natsume, Y., Sugitani, Y., Yamanaka, H., Kuretake, S., … Noda, T. (2002). Lack of acrosome formation in mice lacking a Golgi protein, GOPC. *Proc Natl Acad Sci USA*, *99*, 11211–11216. https://doi.org/10.1073/pnas.162027899

SUPPORTING INFORMATION

Additional supporting information may be found in the online version of the article at the publisher's website.

How to cite this article: Bizkarguenaga, M., Gomez-Santos, L., Madrid, J. F., Sáez, F. J., & Alonso, E. (2022). Zona Pellucida sperm-binding protein 3 receptor distribution during *Gopc*$^{-/-}$ globozoospermic spermatogenesis. *Microscopy Research and Technique*, *85*(4), 1454–1464. https://doi.org/10.1002/jemt.24009